Skin and lung fibrosis induced by bleomycin in mice: a systematic review

S. Gülle[1,2], A. Çelik[2], M. Birlik[1], O. Yılmaz[2]

[1]Division of Rheumatology, Department of Internal Medicine, Dokuz Eylul University School of Medicine, Izmir, Turkey;
[2]Department of Laboratory Animal Science, Dokuz Eylul University School of Medicine, Izmir, Turkey

SUMMARY

Objective. Scleroderma, or systemic sclerosis (SSc), is a chronic autoimmune connective disease with an unknown etiology and poorly understood pathogenesis. The striking array of autoimmune, vascular, and fibrotic changes that develop in almost all patients makes SSc unique among connective tissue diseases. Although no animal model developed for SSc to date fully represents all features of human disease, some animal models that demonstrate features of SSc may help to better understand the pathogenesis of the disease and to develop new therapeutic options. In this review, we aimed to evaluate skin fibrosis and lung involvement in a bleomycin (BLM)-induced mouse model and to evaluate the differences between studies.

Methods. A systematic literature review (PRISMA guideline) on PubMed and EMBASE (until May 2023, without limits) was performed. A primary literature search was conducted using the PubMed and EMBASE databases for all articles published from 1990 to May 2023. Review articles, human studies, and non-dermatological studies were excluded. Of the 38 non-duplicated studies, 20 articles were included.

Results. Among inducible animal models, the BLM-induced SSc is still the most widely used. In recent years, the measurement of tissue thickness between the epidermal-dermal junction and the dermal-adipose tissue junction (dermal layer) has become more widely accepted.

Conclusions. In animal studies, it is important to simultaneously evaluate lung tissues in addition to skin fibrosis induced in mice by subcutaneous BLM application, following the 3R (replacement, reduction, and refinement) principle to avoid cruelty to animals.

Key words: *Scleroderma, murine, bleomycin, skin thickness, pulmonary fibrosis, animal model.*

Reumatismo, 2024; 76 (1): 11-20

INTRODUCTION

Systemic sclerosis (SSc) is a connective tissue disease characterized by microangiopathy, diffuse organ fibrosis, and significant immunological changes, including antibodies specific to nuclear proteins. The heterogeneous nature of the disease is revealed by the variable phenotype and the diversity in the involvement of the visceral organs. Despite the increasing number of studies in the field of SSc, the pathogenesis of this potentially life-threatening disease is still not fully understood.

SCLERODERMA PATHOPHYSIOLOGY

A growing body of evidence suggests that SSc fibrosis is caused by an initial tissue injury, which is followed by the release of inflammatory cytokines, free radicals, and vasoactive mediators, all of which activate immune, fibroblastic, and endothelial cells. Differentiation of stromal cell types into profibrotic myofibroblasts results in a dense accumulation of extracellular matrix and fibrosis. The SSc pathogenesis is based on complex interactions between immune cells, endothelial cells, and fibroblasts. So far, animal models have been used in conjunction with *ex vivo* and *in vitro* data from patients to better understand the mechanisms involved in the development of this condition as well as to uncover new therapeutic targets.

Arteriolar stenosis, capillary dilatation, and capillary loss are structural abnormalities that can be linked to compromised vasculo-

Corresponding author:
Semih Gülle
Division of Rheumatology,
Department of Internal Medicine,
Dokuz Eylul University School of Medicine,
Izmir, Turkey
E-mail: semih.gulle@hotmail.com

genesis and reduced angiogenesis. The altered expression of cell adhesion molecules that cause Th2 and Th17 cells, mast cells, and macrophages infiltration, as well as endothelial dysfunction, which is predominantly caused by low nitric oxide, are examples of functional abnormalities. Intravascular fibrin deposits are induced by activated endothelial-mesenchymal transition, which also results in excessive generation of reactive oxygen species and fibro-proliferative vascular alteration and tissue fibrosis (1).

The accumulation of predisposing factors in immune cells, vascular cells, and interstitial fibroblasts results in phenotypic alterations due to the combination of genetic factors and environmental effects. This leads to vascular activation and structural abnormalities, which in turn cause chronic inflammation and the activation of interstitial fibroblasts derived from different sources (2).

Interstitial fibroblasts in several organs eventually become constitutively activated as a result of these vascular alterations. They also potentiate tissue inhibitors of metalloproteinase-1, prevent the synthesis of collagenases like metalloproteinase (MMP)1 and MMP3, and stimulate transforming growth factor-β (TGFβ) production, fibroblast proliferation, and differentiation. These actions result in an increase in extracellular matrix formation. TGFβ participates in several signaling pathways that encourage fibrogenic and inflammatory effects in people with sickle cell disease. It can also trigger mitogen-activated protein kinase-mediated signaling *via* c-Jun N-terminal kinase, p38, and extracellular signal-regulated kinases 1 and 2. It phosphorylates SMAD proteins, resulting in SMAD4-mediated gene expression (3).

Janus (JAK) kinases are triggered when interleukin (IL)-6 and similar cytokines connect to surface receptors, phosphorylating tyrosine residues in the receptor's cytoplasm (4, 5). According to recent research, SSc biopsies, disease models, and SSc fibroblasts all exhibit substantial JAK/signal transducers and activators of transcription (STAT) activation (6-8). Studies of SSc transcriptomes showed significantly higher levels of expression of a consensus IL6/JAK/STAT3, based on the experimentally derived gene. Furthermore, immunohistochemistry similarly revealed the presence of activated JAKs and activated STAT3 in SSc skin and lung biopsies (9). STAT3 protein appears to contribute to lung fibrosis when activated in lung fibroblasts and alveolar type II cells.

Several inducible or genetic animal models are currently available to study one or more aspects of the disease, but few of them combine all the features of this complex human condition at the same time. Among these models, the tight skin models (TSK-1 and TSK-2) or the bleomycin (BLM)-induced scleroderma model have been described and extensively studied in the last two decades.

Understanding the pathogenesis of SSc is difficult, possibly due to the unique triad of autoimmune/vascular/fibrotic features and the marked heterogeneity of clinical manifestations from one individual to another. It is not surprising that no animal model of SSc has been established reproducing the human disease.

METHODS

Study design

A systematic search was undertaken in the PubMed and Embase databases from inception to May 2023. The medical subject headings (MeSH) used for the search were as follows: ("scleroderma" OR "SSc") AND ("systemic sclerosis") AND ("bleomycine" OR "skin thickness" OR "pulmonary fibrosis"). The following keywords were used with the MeSH terms: ("scleroderma" OR "SSc"), ("systemic sclerosis, skin thickness, murine, animal model, mouse, lung fibrosis"), and ("bleomycine induced skin fibrosis" OR "bleomycine induced lung fibrosis" OR "sclerosis"). Titles and abstracts identified were screened by two of the authors. A manual search of secondary sources included personal holdings, conference abstracts, and a review of the references to identified articles. Figure 1 shows the study flow as recommended by the PRISMA 2020 updated guideline (10).

RESULTS

The search of the four electronic databases identified 316 records (165 from EMBASE, 104 from PubMed, 11 from Cochrane, and 36 from Scopus). By screening titles and abstracts, 278 articles were excluded for duplication and methodological issues. Of the 38 remaining papers, 23 articles were retrieved and 15 were excluded because of abstracts, conference papers, or letters. The full-text screening was performed for 23 articles, with 3 excluded because they had not included outcomes of interest or scleroderma-specific data. No additional article was found after searching the references to the review articles. A total of 20 studies were included in our review.

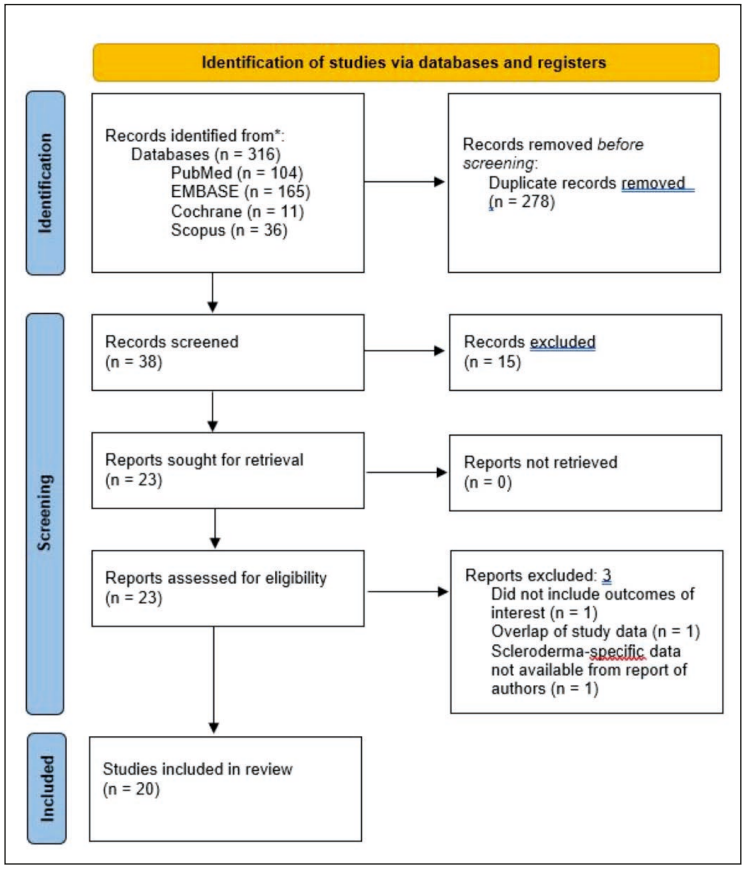

Figure 1 - Study flow diagram.

Mouse model of scleroderma

BLM (11), an antibiotic and antitumor agent, is widely used to induce fibrosis in various organs of rodents. Subcutaneous (SC) BLM injection is associated with early inflammation, with a striking accumulation of monocytes, particularly in the dermis at the injection site (12-14). The inflammatory infiltrate also contains mast cells and sparse eosinophils (15). Progressive dermal fibrosis develops after daily SC (the more commonly used method) or intradermal injections for 1-2 weeks. Simultaneous changes in lung tissue were also observed in mice injected with BLM intraperitoneally (16). These mice showed a rich infiltration of mononuclear cells and fibroblasts, resulting in pulmonary fibrosis. Similar lesions have been reported in the lungs of rabbits who underwent intratracheal BLM (17). The occurrence of interstitial pulmonary fibrosis in athymic nude mice receiving BLM demonstrated that the involvement of immunocompetent cells is not required for fibrosis development and may be the result of direct BLM action on connective tissue-forming cells (18, 19).

In the study of Mountz et al. (12), it was shown that mice injected with non-lethal doses of BLM developed severe dermal fibrosis and hyperpigmentation and had abnormalities in the structure of dermal collagen fibers. However, unlike in human SSc, the presence of only minimal inflammatory changes in the skin without lymphocytic infiltration and negative antinuclear antibodies were the main differences. At this stage, the damaged dermis has thickened and become relatively acellular with excessive collagen accumulation. The hardened lesion remains highly localized and may persist for at least 6 weeks after the last BLM application. Fibroblasts in the lesioned dermis show high expression of Hsp47 (20), a marker for ongoing collagen synthesis, and activation of the intracellular TGF-β/Smad signaling pathway (14). Many fibroblasts stain positive for α-smooth muscle actin, indicating that they have transdifferentiated into smooth muscle-like myofibroblasts (21). Inducible mouse models are used for cancer-related research, the creation of inflammation, immunological models, and infection research (22, 23). Among the current induced mouse models, one of

the most frequently used is the BLM-induced SSc mouse model (24).

Pulmonary fibrosis as a result of subcutaneous administration

Skin and lungs are more susceptible to BLM than other organs, as they have low activity of BLM hydrolase, a cytosolic aminopeptidase (25). Almost all of the fibrosis models induced by BLM in mice are obtained by SC BLM administration. Although serious fibrosis development is observed in a localized area of the skin tissue targeted by SC BLM, it causes SSc-like fibrotic processes also in other distant tissues (especially the lung) as an effect of BLM entering the systemic circulation. Therefore, SC BLM causes infiltration of activated inflammatory cells that secrete cytokines and chemokines in the skin and lung, leading to disruption of the healing process and ultimately accelerating fibrosis (26). A very recent study demonstrated the development of skin thickening and concomitant pulmonary fibrosis following the implantation of mini-osmotic pumps with BLM (Table I) (9, 13, 21, 27-33).

Table I - Bleomycin-induced mouse scleroderma models (skin and lung fibrosis concurrently).

Author (year)	Mouse strain, age	Gender	BLM dose/route/ interval/time	Sacrification day	Pathological specimens	Skin thickness measurement	Concurrent lung fibrosis
Wang et al. (2020) (9)	C57BL/6, 8 wk	F	10 mg/kg/d/SC/2 wk/5 days a week	22	Lesioned back skin	Epidermal-dermal junction to the dermal-fat junction	Present
Marangoni et al. (2022) (28)	C57BL/6 ve C57BL/J (WT), 6 wk	F	10 mg/kg/SC/2 wk/ everyday	15	Lesioned back skin	Epidermal-dermal junction to the dermal-fat junction	Present
Zhao et al. (2019) (29)	C57BL/6 (WT), 8-12 wk	n.a.	10 mg/kg/ID/every other day/4 wk	28	Lesioned back skin	Epidermal-dermal junction to the dermal-fat junction	Present
Ravanetti et al. (2021) (30)	C57BL/6, 7-8 wk	F	60 U/kg (total dose)/ miniosmotic pump (SC)/continuously/7 day	28	Area away from injection, left gluteus	Epidermal-dermal junction to the dermal-fat junction and hypodermis separately and inflammation score	Present
Liang et al. (2015) (31)	C57BL/6 (WT), 6-8 wk	n.a.	150 mg/kg (total dose)/miniosmotic pump (SC)/ continuously/1-4 wk	29	Back skin away from injection	Epidermal-dermal junction to the dermal-fat junction	Present
Ishikawa et al. (2009) (32)	dişi C3H/HeJ, BALB/c and BALB/c nude, 6 wk	F	1 mg/mL/SC/5 days a week/3 wk	22	Lesioned back skin	The ratios between healthy dermal tissues and model dermal tissues were evaluated.	Absent
Yamamoto et al. (2002) (21)	C3H, 6 wk	F	100 µL/SC/every other day/3 wk	22	Lesioned back skin	n.a	Present
Yamamoto et al. (2000) (33)	Balb/c C3H/ He, C57BL/6J, DBA/2, A/J, B10.BR, B10.A and B10.D2, 6 wk	F	1 mg/mL/SC/5 days a week/4 wk	29	Lesioned back skin	Epidermis+dermis	Present
Yamamoto et al. (1999) (13)	BALB/C and C3H, 6 wk	F	1 mg/mL/SC/5 days a week/4 wk	Consecutive follow-up with punch biopsy at week 4 and every other week	Lesioned back skin	Epidermal-dermal junction to the dermal-fat junction	Present

BLM, bleomycin; n.a., not applicable; wk, week; SC, subcutaneously; ID, intradermally; F, female; M, male; WT, wild type.

Skin thickness measurement

Skin fibrosis and increased thickness are important outcomes of the studies. Therefore, objective and repeatable measurements of dermal thickness increase in animal models are critical. In the majority of studies, skin sections were taken at or near the SC application site. Skin thickness is defined as the distance measured under light microscopy between the line connecting adipose tissue and dermis and the line connecting epidermis and dermis (dermal thickness).

However, in some studies, it was calculated as the distance between the epidermis and the line between the connective tissue under the dermal layer. Since dermal thickness measurements are performed using different methods, it is not always possible to compare the results. In recent years, the measurement of tissue thickness between the epidermal-dermal junction and the dermal-adipose tissue junction (dermal layer) has become more widely accepted (Table II) (14, 34-43).

Evaluation of skin thickness measurement accompanied by microscopic images *in vitro* provides a one-time measurement opportunity, and dynamic monitoring of changes in animal skin during the study process is not possible. There are also methods involving serial sacrification of animals for this purpose, to evaluate time-dependent changes.

In vivo *ultrasonic biomicroscopy*

High-frequency ultrasound (range 20-100 MHz) is used in mouse imaging with a fixed-focus mechanical sector scanning head or multifocal electric probes. The choice of ultrasound frequency and probe type represents the trade-off between image resolution and depth of penetration. These transducers allow high-resolution imaging and have mechanical support to perform the micromotions required for mouse studies.

To improve animal welfare across Europe, the European Union has published new guidelines for the protection of laboratory animals according to the 3Rs concept (reduce, refinement, replacement) (44, 45). These guidelines aim to reduce the number of animals used in experiments as much as possible. Therefore, the importance of developing non-invasive measurements of skin involvement in research has emerged. Unlike histological evaluation, ultrasonography (US) does not require sacrificing animals. In particular, high-frequency US is a promising tool in the evaluation and monitoring of oncological, infectious, and inflammatory skin diseases (46-51). In addition to measuring skin thickness in clinical and preclinical studies, it allows a qualitative assessment of the skin *in vivo* (47, 49, 51). Measurement of skin involvement in patients with SSc is essential for diagnosis and prognosis and can be used as a clinical trial outcome measure (52). Currently, skin fibrosis is evaluated with a semi-quantitative score that is limited by intraobserver and interobserver variability (53).

In recent years, with the advances in ultrasound biomicroscopy (UBM) technology, dermal thickness measurement in mouse models can be performed *in vivo* without animal loss. Previous studies demonstrated that fibrosis can be appreciated by observation and palpation of the skin to which BLM was applied. Subsequent papers indicated that skin thickness detected by palpation could be measured quantitatively with UBM (54). In current studies, dermal thickness measurements with UBM before injection, during the study period, and just before sacrification show a close correlation with the histopathological evaluation in TSK-1 mice. In the models created with BLM, a correlation has been found only in a small number of studies (55). This result seems to be related to the technical differences of the models, although the number of studies on this subject is limited.

Computed tomography imaging of pulmonary fibrosis

Micro-computed tomography (CT)-based quantitative tools are used in various animal models to understand the pathogenesis of lung diseases. These methods are aimed at evaluating the disease progression in mice in line with the 3Rs (56-59). Unfortunately, despite this technology's power and potential in preclinical research, there is still little

Table II - Bleomycin-induced mouse scleroderma models (skin fibrosis).

Author (year)	Mouse strain, age	Gender	BLM Dose/route/ time/interval	Sacrification day	Pathological specimens	Skin thickness measurement
Xu et al. (2018) (34)	C57BL/6, 8 wk	F	0.3 mg/mL/SC/every day/3 wk	22	Lesioned back skin	Epidermis+dermis
Rosa et al. (2021) (35)	C57BL/6, 6 wk	M	100 µg/mL/SC/every other day/4 wk	28	Lesioned back skin (1 cm2)	Dermal-epidermal junction and the dermal fibrous connective tissue junction
Jun et al. (2012) (36)	C3H/He, 7 wk	n.a.	Methyl Cellulose-BLM/ SC/once weekly/4 wk	28	Lesioned back skin	Epidermal-dermal junction to the dermal–fat junction
Kanno et al. (2007) (37)	a2AP-deficient (a2AP)/)) and wild-type (a2AP+/+) mice C57BL/6J, 7 wk	M	100 µg/mL/SC/every day/3 wk	22	Lesioned back skin	Epidermal-dermal junction to the dermal–fat junction
Yamamoto et al. (2017) (38)	C3H/He, A/J, DBA2, B10.D2, B10.A, Balb/c, 4-6 wk	F&M	100 µg/mL/ID/every other day/4 wk	29	Lesioned back skin	Epidermal-dermal junction to the dermal-fat junction and hypodermis separately and inflammation score
Ruzehaji et al. (2015) (39)	Balb/C, C57BL/6, DBA/2, 6 wk	F&M	0.5-1 mg/mL/SC/every other day/3 wk	21	Lesioned back skin (1 cm2)	Epidermal-dermal junction to the dermal-fat junction
Oi et al. (2004) (40)	B10.A, C3H/HeJ, C57BL/6J, DBA/2, ve BALB/c, 6 wk	F	1 mg/mL/SC/every other day/4 wk	28	Lesioned back skin (1 cm2)	n.a.
Shibusawa et al. (2008) (41)	C3H, 8 wk	F	poly(L-lactic acid) microspheres/SC/ single dose induction method	7 and 21	Lesioned back skin	n.a.
Yamamoto et al. (2004) (42)	Balb/c nude, 4 wk	F	100 µL/SC/every other day/6 wk	6 wk	Lesioned back skin	Epidermal-dermal junction to the dermal-fat junction
Błyszczuk et al. (2019) (43)	C57BL/6, 6 wk	M	1 mg/mL/SC/every other day / 4 wk	29	Lesioned back skin (1 cm2)	Epidermal-dermal junction to the dermal-fat junction
Takagawa et al. (2003) (14)	C3H, 6 wk	F	1 mg/mL/SC/every day/3 wk	21	Lesioned back skin (1 cm2)	Epidermal-dermal junction to dermal-fat junction

BLM, bleomycin; n.a.,not applicable; wk, week; sc, subcutaneously; id, intradermally; F, female; M, male.

data on quantitative assessment with CT and no clear guidelines for the mouse lung (60-62). To date, no clear predictive densitometry value has been proposed for both the identification and quantification of lung abnormalities such as fibrosis and emphysema in animal models. To the best of our knowledge, investigators' use of Hounsfield Unit ranges to describe different ventilated lung chambers varies depending on animal species or disease (63, 64).

The characteristics of mouse scleroderma models created by BLM induction in the studies mentioned are summarized in the Tables 1 and 2 (9, 13, 14, 21, 28-43).

DISCUSSION AND CONCLUSIONS

Traditionally, a daily SC injection of BLM for 4-6 weeks is commonly used to create a mouse model of SSc. This model, however,

has significant drawbacks, including limited lung involvement, variable skin lesions, and the need for repeat procedures. Although intravenous or intraperitoneal injection of BLM causes SSc-like changes in mice, particularly lung fibrosis, it has a high mortality rate. Therefore, the most appropriate protocols for achieving the desired outcome in the study to create an SSc mouse model must be chosen. The modified protocol of standard 4-week SC BLM administration describes an important method for creating reproducible SSc-interstitial lung disease (ILD) and SSc-skin models in mice through dose-regulated BLM application, with daily weight gain and physiological measurements of mice.

With common experimental conditions in the BLM-mouse model, *i.e.*, injection into a small area of 1 cm^2, the irritating effect of epilation can affect histological results (65, 66). The majority of studies to date have evaluated fibrosis in skin sections taken near the injection site. Although this method contributed significantly to our understanding of fibrotic processes, the local irritation effect in the area where the drug is applied creates a risk of bias in the histopathological evaluation. For this reason, it has been defined as a viable method to collect skin samples from a distant area of the injection site in mice given BLM *via* continuous low-dose SC BLM injection and a mini-osmotic pump, both of which have become common in recent years.

Existing studies in mice provide additional support for the use of US for measuring skin thickness in SSc patients in the clinic. The coordinated use of ultrasound in preclinical mouse studies and clinical trials for the assessment of skin thickening following the application of potential therapeutics will also help evaluate therapeutic efficacy. Skin layers measured with UBM provide the same success as histological studies, which can be difficult for technical reasons (54, 67-69).

When the SSc-ILD-like mouse model is obtained with SC BLM administration, its lung involvement inevitably has significant differences from that obtained by IT and OF administration (70, 71). In the IT instillation technique, the solution is forced by constant pressure and therefore can randomly reach the right or left lung. These applications show a predominantly heterogeneous distribution in the right and left bronchi of the lung and stimulate the development of a direct application-related inflammatory response and severe fibrosis. In SC BLM application, the systemic toxic effect of BLM stimulates a more homogeneous and mild inflammatory response and fibrosis formation in the subpleural areas of the lungs, unlike other methods. Furthermore, compared to the lung changes caused by IT BLM, continuous SC BLM resulted in much more extensive and homogeneous pleural involvement (27). It is also important to adhere to the main "3R principle" of replacement, refinement, and reduction, as this can reduce the number of animals used in research (72, 73).

There have been few studies in animal models of SSc that suggest that high-frequency US may be useful in detecting skin thickening throughout the disease (69). It allows for an *in vivo* qualitative assessment of the skin in addition to measuring skin thickness (47, 49, 51). Measurement of skin involvement in patients with SSc is essential for diagnosis and prognosis and can be used as a clinical trial outcome measure (52). Currently, skin fibrosis is assessed with a semi-quantitative score that is limited by intra- and inter-observer variability (53). Therefore, more objective and sensitive tools to measure skin involvement, such as UBM, are still needed in clinical practice.

In conclusion, the mouse SSc model created by BLM induction is the preferred method for investigating the characteristics of skin and lung involvement. Demonstration of skin and lung fibrosis in SSc mouse models induced by BLM SC administration (direct or continuous SC infusion with an osmotic pump) is useful in the detailed evaluation of SSc.

Contributions

SG, had a substantive role in drafting the final manuscript. The authors directly contributed to the planning, execution, analysis, or report of this scientific article and

approved its final version. The authors are fully responsible for all the content and editorial decisions; the authors involved themselves at all stages of manuscript development and approved the final version.

Conflict of interest
The authors do not have any conflict of interest.

Ethics approval and consent to participate
Not applicable.

Funding
No specific funding was received from any bodies in the public, commercial, or not-for-profit sectors to carry out the work described in this article.

Availability of data and materials
Data are available from the corresponding author upon request.

Acknowledgments
The authors would like to thank Dr. Osman Yılmaz and Dr. Merih Birlik for providing medical writing support.

REFERENCES

1. Jimenez SA, Piera-Velazquez S. Endothelial to mesenchymal transition (EndoMT) in the pathogenesis of Systemic Sclerosis-associated pulmonary fibrosis and pulmonary arterial hypertension. Myth or reality?. Matrix Biol 2016; 51: 26-36.
2. Sierra-Sepúlveda A, Esquinca-González A, Benavides-Suárez SA, Sordo-Lima DE, Caballero-Islas AE, Cabral-Castañeda AR, et al. Systemic sclerosis pathogenesis and emerging therapies, beyond the fibroblast. Biomed Res Int 2019; 2019: 4569826.
3. Morris E, Chrobak I, Bujor A, Hant F, Mummery C, ten Dijke P, et al. Endoglin promotes TGF-β/Smad1 signaling in scleroderma fibroblasts. J Cell Physiol 2011; 226: 3340-8.
4. Schwartz DM, Kanno Y, Villarino A, Ward M, Gadina M, O'Shea JJ. JAK inhibition as a therapeutic strategy for immune and inflammatory diseases. Nat Rev Drug Discov 2017; 16: 843-62. Erratum: Nat Rev Drug Discov 2018; 17: 78.
5. Johnson DE, O'Keefe RA, Grandis JR. Targeting the IL-6/JAK/STAT3 signalling axis in cancer. Nat Rev Clin Oncol 2018; 15: 234-48.
6. Chakraborty D, Šumová B, Mallano T, Chen CW, Distler A, Bergmann C, et al. Activation of STAT3 integrates common profibrotic pathways to promote fibroblast activation and tissue fibrosis. Nat Commun 2017; 8: 1130.
7. Pedroza M, Le TT, Lewis K, Karmouty-Quintana H, To S, George AT, et al. STAT-3 contributes to pulmonary fibrosis through epithelial injury and fibroblast-myofibroblast differentiation. FASEB J 2016; 30: 129-40.
8. Dees C, Tomcik M, Palumbo-Zerr K, Distler A, Beyer C, Lang V, et al. JAK-2 as a novel mediator of the profibrotic effects of transforming growth factor β in systemic sclerosis. Arthritis Rheum 2012; 64: 3006-15.
9. Wang W, Bhattacharyya S, Marangoni RG, Carns M, Dennis-Aren K, Yeldandi A, et al. The JAK/STAT pathway is activated in systemic sclerosis and is effectively targeted by tofacitinib. J Scleroderma Relat Disord 2020; 5: 40-50.
10. Page MJ, McKenzie JE, Bossuyt PM, Boutron I, Hoffmann TC, Mulrow CD, et al. The PRISMA 2020 statement: an updated guideline for reporting systematic reviews. Syst Rev 2021; 372: n71.
11. Adamson IY. Drug-induced pulmonary fibrosis. Environ Health Perspect 1984; 55: 25-36.
12. Mountz JD, Minor MBD, Turner R, Thomas MB, Richards F, Pisko E. Bleomycin-induced cutaneous toxicity in the rat: analysis of histopathology and ultrastructure compared with progressive systemic sclerosis (scleroderma). Br J Dermatol 1983; 108: 679-86.
13. Yamamoto T, Takagawa S, Katayama I, Yamazaki K, Hamazaki Y, Shinkai H, et al. Animal model of sclerotic skin. I: local injections of bleomycin induce sclerotic skin mimicking scleroderma. J Invest Dermatol 1999; 112: 456-62.
14. Takagawa S, Lakos G, Mori Y, Varga J, Yamamoto T, Nishioka K. Sustained activation of fibroblast transforming growth factor-β/smad signaling in a murine model of scleroderma. J Invest Dermatol 2003; 121: 41-50.
15. Yamamoto T, Takahashi Y, Takagawa S, Katayama I, Nishioka K. Animal model of sclerotic skin. II. Bleomycin induced scleroderma in genetically mast cell deficient WBB6F1-W/W(V) mice. J Rheumatol 1999; 26: 2628-34.
16. Adamson IY, Bowden DH. The pathogenesis of bleomycin-induced pulmonary fibrosis in mice. Am J Pathol 1974; 77: 185-97.
17. Laurent GJ, McAnulty RJ, Corrin B, Cockerill P. Biochemical and histological changes in pulmonary fibrosis induced in rabbits with intratracheal bleomycin. Eur J Clin Invest 1981; 11: 441-8.
18. Szapiel S V, Elson NA, Fulmer JD, Hunninghake GW, Crystal RG. Bleomycin-induced interstitial pulmonary disease in the nude, athymic mouse. Am Rev Respir Dis 1979; 120: 893-9.

19. Clark JG, Starcher BC, Uitto J. Bleomycin-induced synthesis of type I procollagen by human lung and skin fibroblasts in culture. Biochim Biophys Acta 1980; 631: 359-70.
20. Sasaki H, Sato T, Yamauchi N, Okamoto T, Kobayashi D, Iyama S, et al. Induction of heat shock protein 47 synthesis by TGF-β and IL-1β via enhancement of the heat shock element binding activity of heat shock transcription factor 1. J Immunol 2002; 168: 5178-83.
21. Yamamoto T, Nishioka K. Animal model of sclerotic skin. V: increased expression of α-smooth muscle actin in fibroblastic cells in bleomycin-induced scleroderma. Clin Immunol 2002; 102: 77-83.
22. Jeong JH. Inducible mouse models for cancer drug target validation. J Cancer Prev 2016; 21: 243-8.
23. Paul Chowdhury B, Gorska MM. Modeling asthma in mice using common aeroallergens. Methods Mol Biol 2022; 2506: 1-18.
24. Yamamoto T, Nishioka K. Animal model of sclerotic skin. VI: evaluation of bleomycin-induced skin sclerosis in nude mice. Arch Dermatol Res 2004; 295: 453-6.
25. Lazo JS, Humphreys CJ. Lack of metabolism as the biochemical basis of bleomycin-induced pulmonary toxicity. Proc Natl Acad Sci 1983; 80: 3064-8.
26. King TE, Pardo A, Selman M. Idiopathic pulmonary fibrosis. Lancet 2011; 378: 1949-61.
27. Lee R, Reese C, Bonner M, Tourkina E, Hajdu Z, Riemer EC, et al. Bleomycin delivery by osmotic minipump: similarity to human scleroderma interstitial lung disease. Am J Physiol Lung Cell Mol Physiol 2014; 306: L736-48.
28. Marangoni RG, Datta P, Paine A, Duemmel S, Nuzzo M, Sherwood L, et al. Thy-1 plays a pathogenic role and is a potential biomarker for skin fibrosis in scleroderma. JCI Insight 2022; 7: e149426.
29. Zhao C, Matsushita T, Ha Nguyen VT, Tennichi M, Fujimoto M, Takehara K, et al. CD22 and CD72 contribute to the development of scleroderma in a murine model. J Dermatol Sci 2020; 97: 66-76.
30. Ravanetti F, Ferrini E, Ragionieri L, Khalajzeyqami Z, Nicastro M, Ridwan Y, et al. SSC-ILD mouse model induced by osmotic minipump delivered bleomycin: effect of Nintedanib. Sci Rep 2021; 11: 18513.
31. Liang M, Lv J, Zou L, Yang W, Xiong Y, Chen X, et al. A modified murine model of systemic sclerosis: Bleomycin given by pump infusion induced skin and pulmonary inflammation and fibrosis. Lab Invest 2015; 95: 342-50.
32. Ishikawa H, Takeda K, Okamoto A, Matsuo SI, Isobe KI. Induction of autoimmunity in a bleomycin-induced murine model of experimental systemic sclerosis: an important role for CD4+ T cells. J Invest Dermatol 2009; 129: 1688-95.
33. Yamamoto T, Kuroda M, Nishioka K. Animal model of sclerotic skin. III: histopathological comparison of bleomycin-induced scleroderma in various mice strains. Arch Dermatol Res 2000; 292: 535-41.
34. Xu X, Chen Z, Zhu X, Wang D, Liang J, Zhao C, et al. S100A9 aggravates bleomycin-induced dermal fibrosis in mice via activation of ERK1/2 MAPK and NF-κB pathways. Iran J Basic Med Sci 2018; 21: 194-201.
35. Rosa I, Romano E, Fioretto BS, Guasti D, Ibba-Manneschi L, Matucci-Cerinic M, et al. Scleroderma-like impairment in the network of telocytes/CD34+ stromal cells in the experimental mouse model of bleomycin-induced dermal fibrosis. Int J Mol Sci 2021; 22: 12407.
36. Jun JB, Kim JK, Na YI, Jang SM, Paik SS, Kim YH. A convenient method for producing the bleomycin-induced mouse model of scleroderma by weekly injections using a methylcellulose gel. Rheumatol Int 2012; 32: 1443-7.
37. Kanno Y, Kuroki A, Okada K, Tomogane K, Ueshima S, Matsuo O, et al. α2-antiplasmin is involved in the production of transforming growth factor β1 and fibrosis. J Thromb Haemost 2007; 5: 2266-73.
38. Yamamoto T. Intradermal injections of bleomycin to model skin fibrosis. In: Rittié L (ed.). New York, NY: Springer New York 2017; 43-7.
39. Ruzehaji N, Avouac J, Elhai M, Frechet M, Frantz C, Ruiz B, et al. Combined effect of genetic background and gender in a mouse model of bleomycin-induced skin fibrosis. Arthritis Res Ther 2015; 17: 145.
40. Oi M, Yamamoto T, Nishioka K. Increased expression of TGF-β1 in the sclerotic skin in bleomycin - "susceptible" mouse strains. J Med Dent Sci 2004; 51: 7-17.
41. Shibusawa Y, Negishi I, Tabata Y, Ishikawa O. Mouse model of dermal fibrosis induced by one-time injection of bleomycin-poly(L-lactic acid) microspheres. Rheumatology (Oxford) 2008; 47: 454-7.
42. Yamamoto T, Nishioka K. Possible Role of Apoptosis in the Pathogenesis of Bleomycin-Induced Scleroderma. J Invest Dermatol 2004; 122: 44-50.
43. Błyszczuk P, Kozlova A, Guo Z, Kania G, Distler O. Experimental mouse model of bleomycin-induced skin fibrosis. Curr Protoc Immunol 2019; 126: e88.
44. Russell WMS, Burch RL. The principles of humane experimental technique. Wheathampstead, Hertfordshire, UK: Universities Federation For Animal Welfare1960.
45. Wells DJ. Animal welfare and the 3Rs in European biomedical research. Ann N Y Acad Sci 2011; 1245: 14-6.
46. Akesson A. Longitudinal development of skin involvement and reliability of high frequency

ultrasound in systemic sclerosis. Ann Rheum Dis 2004; 63: 791-6.
47. El-Zawahry MBM, Abdel El-Hameed El-Cheweikh HM, Abd-El-Rahman Ramadan S, Ahmed Bassiouny D, Mohamed Fawzy M. Ultrasound biomicroscopy in the diagnosis of skin diseases. Eur J Dermatol 2007; 17: 469-75.
48. Hesselstrand R, Scheja A, Wildt M, Akesson A. High-frequency ultrasound of skin involvement in systemic sclerosis reflects oedema, extension and severity in early disease. Rheumatology (Oxford) 2008; 47: 84-7.
49. Jasaitiene D, Valiukeviciene S, Linkeviciute G, Raisutis R, Jasiuniene E, Kazys R. Principles of high-frequency ultrasonography for investigation of skin pathology. J Eur Acad Dermatol Venereol 2011; 25: 375-82.
50. Kaloudi O, Bandinelli F, Filippucci E, Conforti ML, Miniati I, Guiducci S, et al. High frequency ultrasound measurement of digital dermal thickness in systemic sclerosis. Ann Rheum Dis 2010; 69: 1140-3.
51. Kleinerman R, Whang TB, Bard RL, Marmur ES. Ultrasound in dermatology: principles and applications. J Am Acad Dermatol 2012; 67: 478-87.
52. Steen VD, Medsger TA. Improvement in skin thickening in systemic sclerosis associated with improved survival. Arthritis Rheum 2001; 44: 2828-35.
53. Clements PJ, Lachenbruch PA, Ng SC, Simmons M, Sterz M, Furst DE. Skin score: a semiquantitative measure of cutaneous involvement that improves prediction of prognosis in systemic sclerosis. Arthritis Rheum 2010; 33: 1256-63.
54. Scheja A, Akesson A. Comparison of high frequency (20 MHz) ultrasound and palpation for the assessment of skin involvement in systemic sclerosis (scleroderma). Clin Exp Rheumatol 1997; 15: 283-8.
55. Elhai M, Jérôme Avouac, Marchiol C, Renault G, Ruiz B, Fréchet M, et al. Performance of skin ultrasound to measure skin involvement in different animal models of systemic sclerosis. Ultrasound Med Biol 2013; 39: 845-52.
56. Moore BB, Lawson WE, Oury TD, Sisson TH, Raghavendran K, Hogaboam CM. Animal models of fibrotic lung disease. Am J Respir Cell Mol Biol 2013; 49: 167-79.
57. Gammon ST, Foje N, Brewer EM, Owers E, Downs CA, Budde MD, et al. Preclinical anatomical, molecular, and functional imaging of the lung with multiple modalities. Am J Physiol Cell Mol Physiol 2014; 306: L897-914.
58. Clark DP, Badea CT. Micro-CT of rodents: state-of-the-art and future perspectives. Phys Med 2014; 30: 619-34.
59. Bidola P, Martins de Souza e Silva J, Achterhold K, Munkhbaatar E, Jost PJ, Meinhardt AL, et al. A step towards valid detection and quantification of lung cancer volume in experimental mice with contrast agent-based X-ray microtomography. Sci Rep 2019; 9: 1325.
60. Saito S, Murase K. Detection and early phase assessment of radiation-induced lung injury in mice using micro-CT. PLoS One 2012; 7: e45960.
61. Ninaber MK, Stolk J, Smit J, Le Roy EJ, Kroft LJM, Els Bakker M, et al. Lung structure and function relation in systemic sclerosis: application of lung densitometry. Eur J Radiol 2015; 84: 975-9.
62. Perez JR, Lee S, Ybarra N, Maria O, Serban M, Jeyaseelan K, et al. A comparative analysis of longitudinal computed tomography and histopathology for evaluating the potential of mesenchymal stem cells in mitigating radiation-induced pulmonary fibrosis. Sci Rep 2017; 7: 9056.
63. Colombi D, Dinkel J, Weinheimer O, Obermayer B, Buzan T, Nabers D, et al. Visual vs fully automatic histogram-based assessment of idiopathic pulmonary fibrosis (IPF) progression using sequential multidetector computed tomography (MDCT). PLoS One 2015; 10: e0130653.
64. Mah K, Van Dyk J. Quantitative measurement of changes in human lung density following irradiation. Radiother Oncol 1988; 11: 169-79.
65. Beyer C, Schett G, Distler O, Distler JHW. Animal models of systemic sclerosis: prospects and limitations. Arthritis Rheum 2010; 62: 2831-44.
66. Yamamoto T. Animal model of systemic sclerosis. J Dermatol 2010; 37: 26-41.
67. Kissin EY, Schiller AM, Gelbard RB, Anderson JJ, Falanga V, Simms RW, et al. Durometry for the assessment of skin disease in systemic sclerosis. Arthritis Rheum 2006; 55: 603-9.
68. Salmhofer W, Rieger E, Soyer HP, Smolle J, Kerl H. Influence of skin tension and formalin fixation on sonographic measurement of tumor thickness. J Am Acad Dermatol 1996; 34: 34-9.
69. Tedstone JL, Richards SM, Garman RD, Ruzek MC. Ultrasound imaging accurately detects skin thickening in a mouse scleroderma model. Ultrasound Med Biol 2008; 34: 1239-47.
70. McDonald B, Spicer J, Giannais B, Fallavollita L, Brodt P, Ferri LE. Systemic inflammation increases cancer cell adhesion to hepatic sinusoids by neutrophil mediated mechanisms. Int J Cancer 2009; 125: 1298-305.
71. Haupt W, Riese J, Mehler C, Weber K, Zowe M, Hohenberger W. Monocyte function before and after surgical trauma. Dig Surg 1998; 15: 102-4.
72. Flecknell P. Replacement, reduction and refinement. ALTEX 2002; 19: 73-8.
73. Tannenbaum J, Bennett BT. Russell and Burch's 3Rs then and now: the need for clarity in definition and purpose. J Am Assoc Lab Anim Sci 2015; 54: 120-32.